ADVANCES IN ATMOSPHERIC SCIENCES, VOL. 29, NO. 3, 2012, 599–610

A Parameterized yet Accurate Model of Ozone and Water Vapor Transmittance in the Solar-to-near-infrared Spectrum

LIU Weiyi* (刘为一) and QIU Jinhuan (邱金桓)

Key Laboratory of Middle Atmosphere and Global Environment Observation,

Institute of Atmospheric Physics, Chinese Academy of Sciences, Beijing 100029

(Received 31 May 2011; revised 23 November 2011)

ABSTRACT

A parameterized transmittance model (PTR) for ozone and water vapor monochromatic transmittance calculation in the solar-to-near-infrared spectrum 0.3–4 μm with a spectral resolution of 5 cm^{-1} was developed based on the transmittance data calculated by Moderate-resolution Transmittance model (MODTRAN). Polynomial equations were derived to represent the transmittance as functions of path length and airmass for every wavelength based on the least-squares method. Comparisons between the transmittances calculated using PTR and MODTRAN were made, using the results of MODTRAN as a reference. Relative root-mean-square error (RMSre) was 0.823% for ozone transmittance. RMSre values were 8.84% and 3.48% for water vapor transmittance ranges of 1–1$\times$10^{-18} and 1–1$\times$10^{-3}, respectively. In addition, the Stratospheric Aerosol and Gas Experiment II (SAGEII) ozone profiles and University of Wyoming (UWYO) water vapor profiles were applied to validate the applicability of PTR model. RMSre was 0.437% for ozone transmittance. RMSre values were 8.89% and 2.43% for water vapor transmittance ranges of 1–1$\times$10^{-18} and 1–1$\times$10^{-6}, respectively. Furthermore, the optical depth profiles calculated using the PTR model were compared to the results of MODTRAN. Absolute RMS errors (RMSab) for ozone optical depths were within 0.0055 and 0.0523 for water vapor at all of the tested altitudes. Finally, the comparison between the solar heating rate calculated from the transmittance of PTR and Line-by-Line radiative transfer model (LBLRTM) was performed, showing a maximum deviation of 0.238 K d^{-1} (6% of the corresponding solar heating rate calculated using LBLRTM). In the troposphere all of the deviations were within 0.08 K d^{-1}. The computational speed of PTR model is nearly two orders of magnitude faster than that of MODTRAN.

Key words: parameterization, transmittance, atmospheric absorption

Citation: Liu, W. Y., and J. H. Qiu, 2012: A parameterized yet accurate model of ozone and water vapor transmittance in the solar-to-near-infrared spectrum. *Adv. Atmos. Sci.*, **29**(3), 599–610, doi: 10.1007/s00376-011-1076-6.

1. Introduction

It is well known that the absorption of atmospheric gases in the solar-to-near-infrared spectrum is 0.3–4 μm, where nearly 95% of the concentrated solar radiation has an important role in determining the solar heating rate and thus affects the Earth's radiation budget (Liou, 2002). Therefore, the absorption of ozone and water vapor in this spectral range is climatically important. Numerous models have been developed for gas absorption and transmittance calculation. The high-resolution transmission molecular absorption database (HITRAN) (Rothman et al., 2005) is a database that contains all known spectral lines of all relevant atmospheric molecules. Line-by-line programs (effectively unlimited spectral resolution) use the HITRAN database to calculate transmittances and radiances for arbitrary atmospheric structures. LBLRTM (Clough et al., 2005) is the most commonly used line-by-line (LBL) program in atmospheric and environmental research. Compared to the LBL method, the low-resolution radiance and transmit-

*Corresponding author: LIU Weiyi, v16v1@hotmail.com

tance model (LOWTRAN 7) (Kneizys et al., 1988) and the moderate-resolution model MODTRAN 5 (Berk et al., 2004) are two faster lower-spectral-resolution (20 cm^{-1} and 0.1 cm^{-1}, respectively) models developed using the band model.

Although the band models have greatly improved operational speed compared to LBL models, more efficient parameterized models are needed to deal with the large quantity of repeated calculations of gas absorption and transmittance. A number of investigators have developed parameterized schemes for gas absorption and transmittance calculations for different gases in different bands, including the ozone absorption and transmittance in the 9.6-μm region (Kiehl and Solomon, 1986; Kratz and Cess, 1988; Rosenfield, 1991; Fu and Liou, 1992), the carbon dioxide (CO_2) absorption and emission in the 15-μm band (Ou and Liou, 1983), and infrared emission and absorption by water vapor (Zhong and Haigh, 1995; Collins et al., 2002). Most of the previous parameterizations have concentrated on the infrared bands. In this study, we developed a parameterized model for the monochromatic transmittance calculation for both ozone and water vapor in solar-to-near-infrared spectrum in the range of 0.3–4 μm, which can be applied to the solar heating rate and radiation transfer calculation in climate models. In our study, based on the database of sufficient transmittance calculations for multiple atmospheric conditions using MODTRAN, the least-squares method was applied to the database to generate the parameterized formulas for ozone and water vapor respectively in every wavelength. In section 2 the data used in our study is described. In section 3 a detailed description of our parameterized model is presented. In section 4 an accuracy analysis on transmittance and solar heating rate results of PTR based on a comparison with MODTRAN and LBLRTM is presented. The evaluation of computational speed is also included. Section 5 presents the conclusion.

2. Data

In this study, the transmittance data of ozone and water vapor calculated by MODTRAN for 6 atmosphere models and 10 solar zenith angles (SZA) in 6166 wavelengths were used to derive the parameterized model. Six atmosphere models include Tropical Atmosphere (TRO), Mid-Latitude Summer Atmosphere (MLS), Mid-Latitude Winter Atmosphere (MLW), Sub-Arctic Summer Atmosphere (SAS), Sub-Arctic Winter Atmosphere (SAW) and U.S. Standard Atmosphere (USS). Ten SZAs used in this study included 0°, 10°, 20°, 30°, 40°, 50°, 60°, 70°, 75°, and 80°. Some 6166 wavelengths corresponded to all of the wavenumbers from 2500 to 33 330 cm^{-1} (wavelengths from 0.3 to 4 μm), with a resolution of 5 cm^{-1}.

The monthly means of ozone profiles provided by SAGEII (Mauldin et al., 1985) and water vapor profiles provided by UWYO were used to examine the applicability of the parameterized model. SAGEII provided global distribution data for aerosol, ozone, water vapor, and nitrogen dioxide over a period of 21 years. The SAGEII water vapor profiles are not reliable because of the lack of records of water vapor content for the lower atmosphere, which accounts for a great proportion of the total vertical water vapor content. Thus, only the ozone profiles were used. UWYO supplied the water vapor profile in North America, Latin America, East Asia, and Middle East daily at 0000 UTC and 1200 UTC. The vertical profiles in North America reached 80 levels, so the profiles in North America were used.

3. The parameterization model

In this section, details of the PTR model are presented. For a single wavelength λ, monochromatic transmittance τ_λ between the top of the atmosphere and any level z in the direction θ from the zenith is given by

$$\tau_\lambda(z) = \exp[-mu_\lambda(z)] \,, \tag{1}$$

where

$$u_\lambda(z) = k_\lambda \int_z^{z_\infty} \rho(z')dz' \,, \tag{2}$$

$u_\lambda(z)$ is the gas optical depth between the top of the atmosphere and level z, m is the airmass, k_λ is the absorption coefficient at wavelength λ, ρ is the density of absorption gas, and z_∞ represents the height of the top of the atmosphere (Liou, 2002). Due to the curvature of the Earth and refraction, θ varies along the path. However, if the zenith angle is $<80°$, the variation of θ along the path is negligible. When zenith angle is $>80°$, the curvature of the Earth and refraction must be taken into account, and airmass can be written in the form

$$m = [\cos\theta + 0.50572(96.07995 - \theta)^{-1.6364}]^{-1} \,, \tag{3}$$

which gives reasonable results for zenith angles of $\leqslant 90°$, with an airmass of $\sim$38 at the horizon (Young, 1994). In our study, the airmass for all of the SZAs are calculated using Eq. (3). The following process of parameterization is based on the fact that monochromatic transmittance τ_λ decreases with increasing airmass and decreases with increasing path length w, which is given by Eq. (4):

$$w(z) = \int_z^{z_\infty} \rho(z')dz' \,. \tag{4}$$

3.1 *Ozone parameterization*

In the parameterization of ozone transmittance, the product of path length w and airmass m is defined as slant path length (SPL). To derive a unique relationship between ozone transmittance and SPL, a series of transmittance and optical depth computations were conducted using MODTRAN for different SZAs for six atmosphere models in the 0.3–4 μm spectral range. The monochromatic transmittances did not change smoothly with SPL, whereas slant optical depths (the product of air mass and optical depth) changed smoothly with the SPL. Hence, there must be a specific function that can approximately represent the relationship between slant optical depths and SPL for every wavelength. Based on the least-squares method, a third-degree polynomial was derived to fit the ozone optical depth, which is given by

$$u_\lambda = m^{-1} \sum_{i=1}^{3} a_{i(\lambda)} (wm)^{i-1} , \qquad (5)$$

where w is the ozone path length; m is the air mass; $a_{1(\lambda)}$, $a_{2(\lambda)}$, and $a_{3(\lambda)}$ are the coefficients for wavelength λ; and u_λ is the ozone optical depth. The ozone transmittance τ_λ can be obtained from Eq. (1).

3.2 *Water vapor parameterization*

For the parameterization of water vapor transmittance, effective water vapor path length (Yang and Qiu, 2002) was adopted as a substitute for water vapor path length in the form

$$w_e(z) = \int_z^{z_\infty} \frac{p}{p_0} \sqrt{\frac{T_0}{T}} \rho(z') dz' , \qquad (6)$$

where p and T are the pressure and temperature for different altitudes, respectively, p_0 is equal to 1013 hPa, T_0 is equal to 273 K, and ρ is the water vapor density. The calculation of the effective path length involves the impact of pressure and temperature so that they need not be taken into account in the calculation of absorption coefficient. Differences between the absorption coefficients for different atmosphere models become smaller, minimizing the error of parameterization.

The relationship between optical depth and SPL of water vapor is more complicated than that of ozone. Figure 1 shows the computed results for SPL $\geqslant$0.3 and $<$0.3 in 1.36 μm as a representative of all of the wavelengths. Curve 1 in Fig. 1b is the same as the fitted curve in Fig. 1a. If we fit all of the points with curve 1, the differences between MODTRAN data and fitted curve are extra large when SPL is $<$0.3. Therefore, the parameterization of water vapor was divided into two parts.

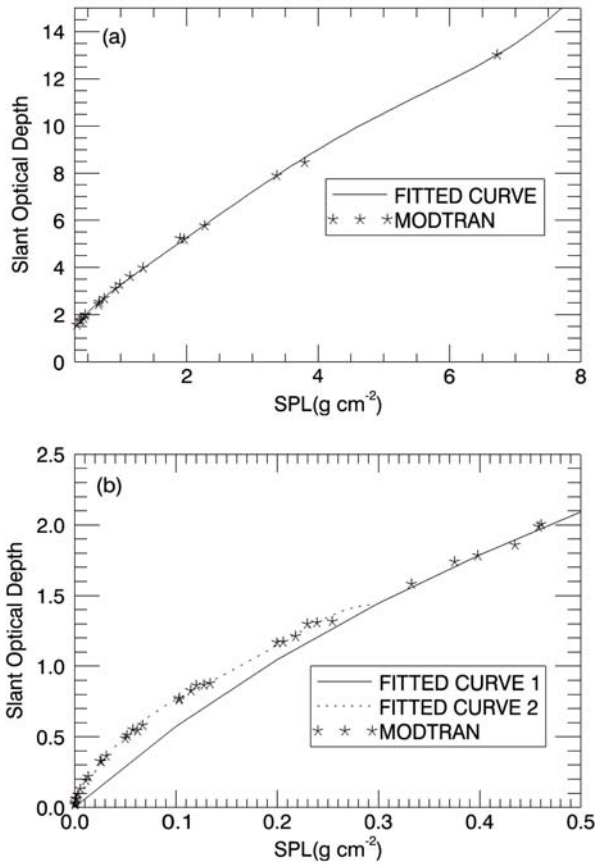

Fig. 1. Water vapor optical depth data calculated using MODTRAN as functions of SPL along with the fitted curves for (a) SPL $\geqslant$ 0.3 and (b) SPL $<$0.3.

3.2.1 *For SPL* $\geqslant$0.3

Changes were made to the optical depth to be fitted as follows. The modified optical depth, called scaled optical depth, is defined as

$$u'_\lambda = u_\lambda / (1 - e^{-2 w_e m}) . \qquad (7)$$

Scaled optical depth is more qualified for the parameterization than optical depth when the SPL is not tiny. The scaled optical depth changes more smoothly with the SPL than the original optical depth, and thus smaller fitting errors can be obtained. However, when SPL is small, this effect is not obvious so we only applied scaled optical depth to the "SPL $\geqslant$ 0.3" case. Base on the least-squares method, a fifth-degree polynomial was derived to fit the scaled optical depths given by

$$u_\lambda / (1 - e^{-2 w_e m}) = (1/m) \sum_{i=1}^{5} a_{i(\lambda)} (w_e m)^{i-1} \qquad (w_e m \geqslant 0.3) , \qquad (8)$$

where $a_{1(\lambda)} - a_{5(\lambda)}$ are the coefficients for wavelength λ. Water vapor transmittance τ_λ can be obtained from Eq. (1).

3.2.2 *For SPL <0.3*

The original optical depths were reused in parameterization. To ensure the continuity of these two curves shown in the figures, the point with an SPL of 0.3 in the curve for SPL $\geqslant$0.3 was added as an extra point to be fitted. Base on the least-squares method, a five-degree polynomial was derived to fit the water vapor optical depth in the form

$$u'_\lambda = (1/m)\sum_{i=1}^{5} a_{i(\lambda)}(w_e m)^{i-1} \quad (w_e m < 0.3)\,. \quad (9)$$

As a result of this process, the parameterized scheme for a single wavelength λ was obtained. By applying the same scheme to all of the 6166 wavelengths in the range of 0.3–4 μm with a spectral resolution of 5 cm^{-1}, we derived the parameterized model for ozone and water vapor monochromatic transmittance calculation in this spectral range.

4. Comparisons and analyses

The accuracy and applicability of PTR model were examined by analyzing the RMSre and RMSab of the parameterized transmittances with reference to their true values (i.e., MODTRAN transmittance being treated as true values in this section). Relative error $E_{\rm re}$ and absolute error $E_{\rm ab}$ are given by

$$E_{\rm re} = |R_{\rm ptr}/R_{\rm true} - 1| \times 100\%\,, \quad (10)$$

$$E_{\rm ab} = |R_{\rm ptr} - R_{\rm true}|\,, \quad (11)$$

where $R_{\rm ptr}$ represents the results of the parameterized model (including transmittance, vertical optical depth, and broadband irradiance), and $R_{\rm true}$ represents the results of MODTRAN. All transmittances analyzed in this section were $>1 \times 10^{-18}$, and correspondingly, all of the slant optical depths were <41.45. In the spectral range of 0.3–4 μm, comparisons were conducted in the range of 0.3–0.8 μm (including 4097 wavelengths) for ozone and in the range of 0.568–4 μm (including 3021 wavelengths) for water vapor because the absorptions of these two kinds of gases are very weak in the wavelengths outside these two bands.

4.1 *Comparison with MODTRAN for ozone transmittance and optical depth*

4.1.1 *Six MODTRAN atmosphere models cases*

We compared the PTR model results with MODTRAN calculated transmittance for 10 SZAs in 6 atmosphere models in the range of 0.3–0.8 μm. The overall comparison is shown in Fig. 2. Most of the points fall on the dashed line with a slope of one. The RMSre between all of the fitted points and the MODTRAN computed points was 0.823%. To achieve more quantitative comparisons, detailed RMSre and RMSab over

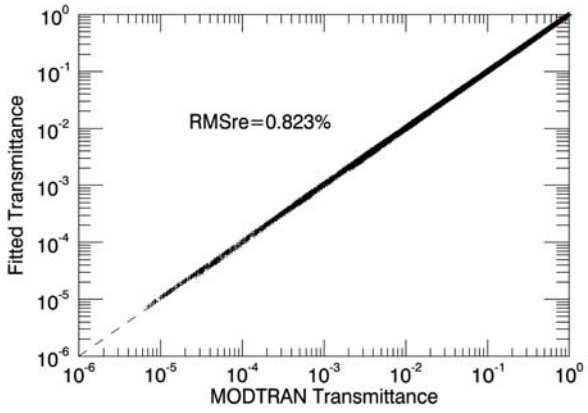

Fig. 2. Comparison between the ozone transmittance calculated using PTR model and MODTRAN. Every point represents a fitted point.

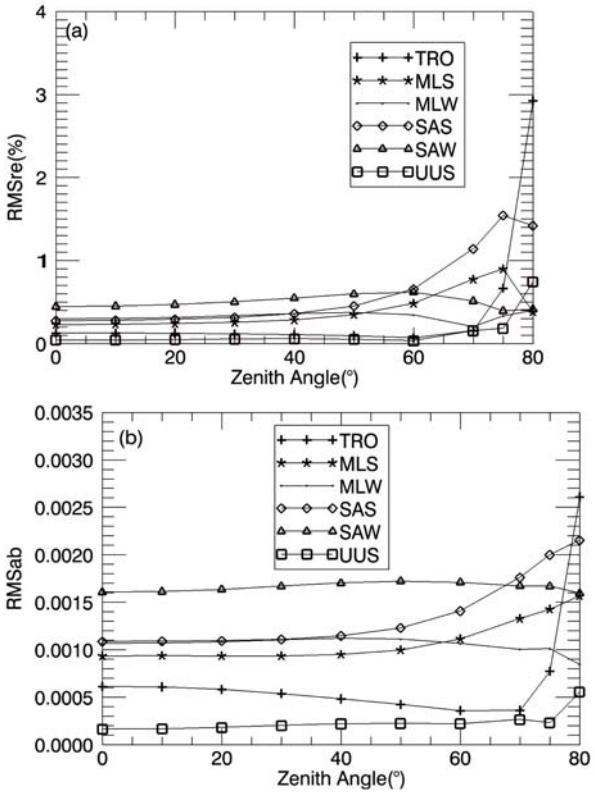

Fig. 3. (a) Relative errors and (b) absolute errors of parameterized ozone transmittance for 10 SZAs and for 6 atmosphere models. Different types of lines represent different atmosphere models.

Table 1. RMS errors of parameterized ozone transmittance of SAGEII monthly mean ozone profiles.

	Ozone Profiles SZA					
	October 1984			July 2005		
	15°	45°	72°	15°	45°	72°
RMSre (%)	0.34	0.41	0.46	0.073	0.14	0.66
RMSab	1.16×10^{-3}	1.12×10^{-4}	4.93×10^{-4}	3.97×10^{-4}	5.76×10^{-4}	1.03×10^{-3}

Table 2. RMS errors of parameterized ozone transmittance and optical depth in MFR and AERONET channels.

	Channel (μm)	Transmittance RMSre (%)	Transmittance RMSab	Optical depth RMSre (%)	Optical depth RMSab
MFR	0.415	1.13×10^{-3}	1.10×10^{-5}	2.03	1.22×10^{-5}
	0.500	0.027	3.01×10^{-4}	0.57	6.13×10^{-5}
	0.615	0.098	9.71×10^{-4}	0.71	2.43×10^{-4}
AERONET	0.340	0.102	9.12×10^{-4}	4.12	4.52×10^{-4}
	0.440	4.03×10^{-3}	3.89×10^{-5}	2.75	2.12×10^{-5}
	0.500	0.025	3.01×10^{-4}	0.67	6.47×10^{-5}
	0.670	0.042	4.12×10^{-4}	0.71	8.97×10^{-5}

all of the wavelengths for 10 SZAs in 6 atmosphere models are presented in Fig. 3. The RMSre increases obviously when SZA is >70°. The increase in relative errors for large SZAs can be explained by the fact that when the SZA is >70° the optical path rapidly increases with increasing SZA thus the transmittance decreases rapidly. However, the RMSab for a large SZA is usually very small. For example, the maximum RMSre is 2.92% with a corresponding RMSab of only 2.61×10^{-3}. The differences between the errors for different atmosphere models (Fig. 3) can be explained by the fact that different gas contents for each model lead to different transmittances. Figure 4 illustrates the detailed RMSre and RMSab for 60 permutations of 10 SZAs and 6 atmosphere models for all of the wavelengths in the range of 0.3–0.8 μm. In most wavelengths, RMSre is <1%, while this error becomes larger when the wavelength approaches 0.3 μm. The increase is mainly caused by the strong absorption by ozone near 0.3 μm that leads to small transmittances in this spectral range. The same is true for the water vapor case below. The corresponding RMSab in these wavelengths are very small. For example, maximum RMSre is 4.12% with a RMSab of only 1.01×10^{-3}, and these errors of ozone transmittance calculation are acceptable.

4.1.2 *SAGEII ozone profiles cases*

The aforementioned comparisons were for the points directly fitted in the process of parameterization. In this section, the accuracy of the PTR model of the points, which were not directly included in the process of parameterization, is taken into account. In addition, monthly means of the SAGEII ozone profiles for October 1984 and July 2005 were adopted instead of the six atmospheric profiles used in parameterization. The transmittances of these two profiles for three SZAs (15°, 45°, and 72°) were calculated, and comparisons between the results of these two models were conducted. The overall RMSre was 0.374% and RMSab was 8.59×10^{-3}. Detailed RMS errors over 4097 wavelengths in the range of 0.3–0.8 μm for every case are listed in Table 1 with all of the RMSre within 1% and RMSab within 0.0012. These comparisons indicate that the ozone transmittance calculations in the points not directly included in the process of parameterization are accurate as well.

4.1.3 *The channels of MFR and AERONET*

The Aerosol Robotic Network (AERONET) (Holben et al., 1998) program is a federation of ground-based sun photometer measurement networks. It started in 1993 at more than a dozen sites and has grown rapidly to more than 100 sites worldwide. A multifilter rotating shadowband radiometers (MFR) (Harrison et al., 1994) is a field instrument that measures the global, direct, and diffused components of solar irradiance at up to seven wavelengths. To show PTR model performance in practical application, comparisons with MOTRAN for transmittance and optical depth in seven commonly used wavelengths are listed in Table 2, including three channels of MFR (415 nm, 500 nm, and 615 nm) and four channels of AERONET (340 nm, 440 nm, 500 nm, and 670 nm). All of the aforementioned channels were within 0.3–0.8 μm. The RMSre (for 60 permutations of 10 SZAs and 6 atmosphere models) of all channels were within 4.12% and 0.11%, and the RMSab were within 1.0×10^{-3} and

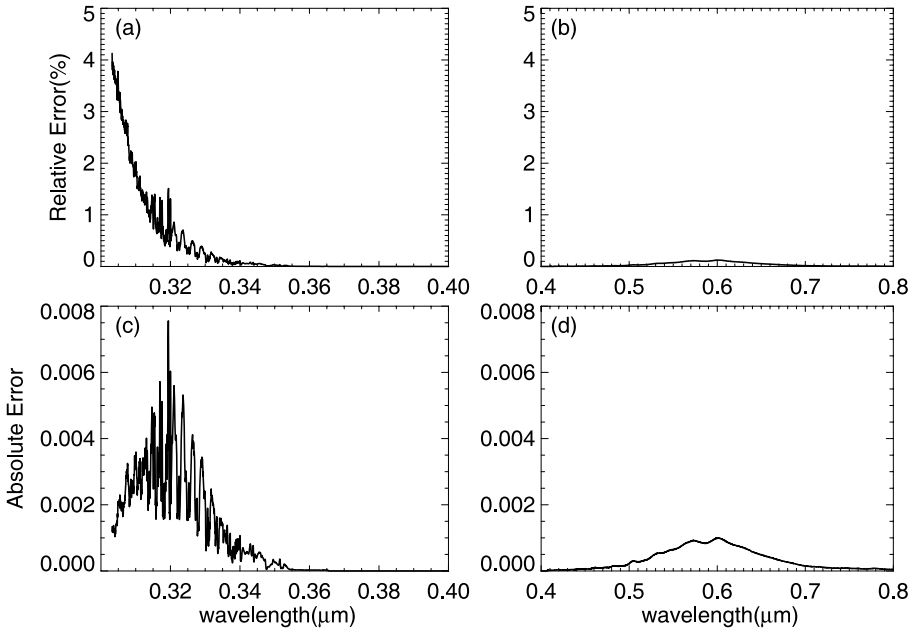

Fig. 4. (a and b) Relative RMS errors. (c and d) Absolute RMS errors of parameterized ozone transmittance for every single wavelength in the range of 0.3–0.8 μm.

4.52×10^{-4} for optical depth and transmittance, respectively.

4.2 *Comparison with MODTRAN for water vapor transmittance and optical depth*

4.2.1 *Six MODTRAN atmosphere models cases*

In this section, we compared PTR model results with MODTRAN calculated transmittances for 10 SZAs in 6 atmosphere models in the range of 0.568–4 μm. First, an overall comparison was conducted (Fig. 5). The RMSre between fitted points and all MODTRAN data points was 8.84% and RMSab was 4.21×10^{-3}. The distance between the points and the dashed line increased with decreasing transmittance, indicating that RMS errors mainly came from small transmittances ($1\times10^{-18}-1\times10^{-3}$). Therefore, when transmittances were constrained within the range of 0.001–1, RMSre decreased to 3.48%. The detailed errors of transmittances for different transmittance intervals in seven water vapor absorption bands and six atmosphere models are listed in Table 3. Although RMSre mainly comes from the transmittance range of

Table 3. RMS errors of parameterized water vapor transmittance for seven water vapor absorption bands and six atmosphere models in four transmittance intervals.

	Transmittance intervals error type				
	1×10^{-3}–1		1×10^{-6}–1×10^{-3}	1×10^{-12}–1×10^{-6}	1×10^{-18}–1×10^{-12}
	RMSab (10^{-3})	RMSre (%)	RMSab (10^{-5})	RMSab (10^{-8})	RMSab (10^{-14})
Center wavelength (μm)					
0.72	0.91	0.112			
0.82	1.03	0.123			
0.94	4.60	1.08			
1.1	4.70	1.31	2.41		
1.38	6.89	5.36	5.34	6.78	6.19
1.87	6.59	4.99	6.03	8.43	10.3
2.7	9.23	6.21	6.43	7.99	6.72
Atmosphere model					
TRO	4.76	4.12	7.12	12.4	12.1
MLS	2.54	1.87	3.21	6.78	6.98
MLW	5.01	3.21	7.54	6.54	6.62
SAS	2.36	1.89	3.65	3.67	8.87
SAW	1.03	6.01	9.89	4.01	6.85
UUS	3.13	2.22	5.01	4.78	9.87

Note: The blank in table indicate that none of the calculated transmittances in the band falls in the transmittance range.

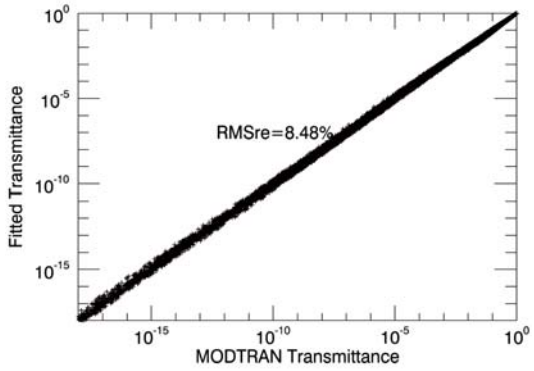

Fig. 5. Comparison between the water vapor transmittance calculated using the PTR model and MODTRAN. Every point represents a fitted point.

1×10^{-18}–1×10^{-3}, the corresponding RMSab in this range is very small. The relative errors of tropical atmosphere were found to be greater than those of other models (Table 3). This is due to the strong evaporation that leads to large optical depths in this region. Figures 6a and b illustrates the detailed errors for transmittances in different wavelengths within the range of 0.568–4 μm. At some wavelengths, RMSre can reach 58%. The large RMSre has two causes. First, wavelengths with large relative errors are usually near the center of the absorption band where the absorption is very strong and transmittances are very small. Second, our original fitted variable was optical depth instead of transmittance, and a very tiny error of optical depth fitting can lead to a large error in the transmittance fitting, especially when optical depth is large. Thus to further illustrate PTR model's accuracy, the errors of water vapor optical depths are presented in Figs. 6c and d as well. The RMSre in most of the wavelengths were within 5% and reached 10% in only a few wavelengths. For wavelengths with large RMSre, the RMSab were always very small. For example, maximum RMSre was 12.1%, with a corresponding RMSab of 0.0016. So the accuracy of water vapor transmittance fitting is acceptable.

4.2.2 *UWYO water vapor profiles cases*

To examine the accuracy of PTR model in the points not fitted directly in the process of parameterization, water vapor profiles at 0000 UTC 11 May 2010 in Green Bay (GRB) and Blacksburg (RNK) were adopted instead of the six atmosphere profiles used in the parameterization. Transmittances for three SZAs (15°, 45°, and 72°) of these two profiles were calculated using the PTR model and MODTRAN in the range of 0.568–4 μm. Overall RMSre for water vapor transmittance is 7.92% and RMSab is 0.0024. RMSre decreased to 2.25% when the transmittance was $>1 \times 10^{-6}$. The detailed RMS errors over 3021 wavelengths in the range of 0.568–4 μm for every case are listed in Table 4, with all of the RMSre within 11.3%

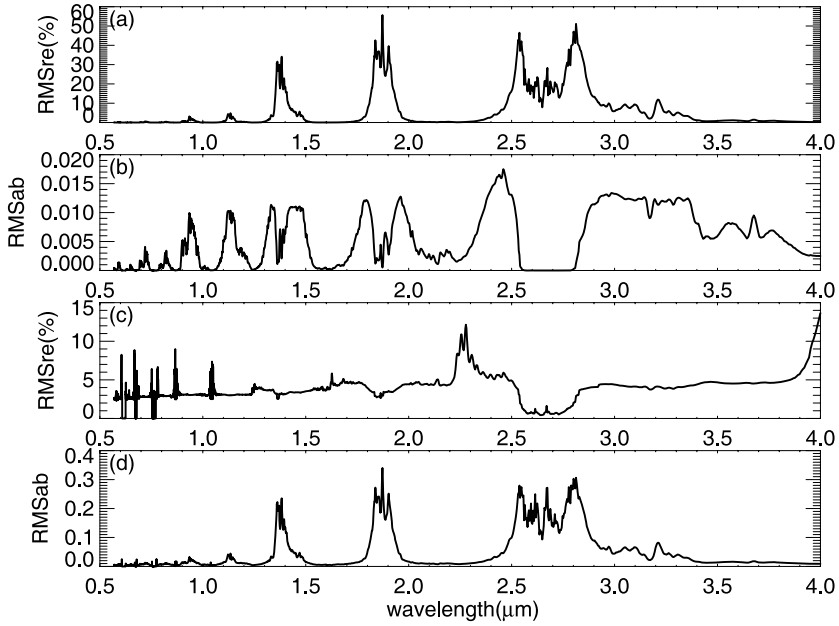

Fig. 6. (a) Relative RMS errors and (b) absolute RMS errors of parameterized water vapor transmittance, as well as (c) relative RMS errors and (d) absolute RMS errors of parameterized water vapor optical depth for every single wavelength in the range of 0.568–4 μm.

Table 4. RMS errors of parameterized water vapor transmittance of UWYO profiles for different transmittance intervals.

	Water vapor profile SZA					
	RNK			GRB		
	15°	45°	72°	15°	45°	72°
RMSre (%)	3.26	9.03	11.23	4.85	8.12	9.87
RMSab	1.88×10^{-3}	2.13×10^{-3}	2.26×10^{-3}	1.89×10^{-3}	2.56×10^{-3}	3.01×10^{-3}
RMSre (%) ($\tau_v > 1 \times 10^{-6}$)	1.79	2.23	1.41	1.47	2.31	3.02
RMSab ($\tau_v > 1 \times 10^{-6}$)	1.90×10^{-3}	2.17×10^{-3}	2.41×10^{-3}	1.97×10^{-3}	2.61×10^{-3}	3.21×10^{-3}

Table 5. RMS errors of parameterized water vapor transmittance and optical depth in MODIS and AERONET channels.

	Channel (μm)	Transmittance RMSre (%)	Transmittance RMSab	Optical depth RMSre (%)	Optical depth RMSab
AERONET	0.670	1.53×10^{-2}	2.71×10^{-5}	3.01	2.01×10^{-5}
	0.870	2.91×10^{-2}	2.57×10^{-5}	4.35	1.67×10^{-5}
	0.940	1.13	6.97×10^{-3}	3.05	8.78×10^{-3}
	0.102	3.12×10^{-2}	3.12×10^{-4}	2.97	2.32×10^{-4}
MODIS	0.890 − 0.920	0.60	4.12×10^{-3}	3.11	4.12×10^{-3}
	0.931−0.941	2.34	8.78×10^{-3}	2.86	1.62×10^{-2}
	0.915−0.965	1.61	7.22×10^{-3}	2.79	1.07×10^{-2}

and RMSab within 3.01×10^{-3}. When transmittances were $>1 \times 10^{-6}$, all of the RMSre were within 3.02%.

4.2.3 *AERONET and MODIS channels*

The performance of the PTR model in AERONET and Moderate Resolution Imaging Spectroradiometer (MODIS) channels inside the range 0.568–4 μm are reported in this section. The wavelengths adopted included three water vapor channels of MODIS (890–920 nm, 931–941 nm, and 915–965 nm) and four channels of AERONET (670 nm, 870 nm, 940 nm, and 1020 nm). Comparisons with MODTRAN for transmittances and optical depths in these wavelengths were conducted, and the errors for these channels are listed in Table 5. (RMS errors for each MODIS channel are the average of all of the RMS errors over the wavelengths inside each channel.) For all of the channels, the RMSre (for 60 permutations of 10 SZAs and 6 atmosphere models) were within 2.34% and 4.35%, and the RMSab were within 0.01 and 0.0162, respectively, for transmittance and optical depth.

4.3 *Comparison with MODTRAN for ozone and water vapor optical depth profiles*

To examine the accuracy of the parameterized model at different altitudes, the calculations for eight altitudes for 6166 wavelengths under six different cases (TRO, UUS, and SAW models with SZA of 0°or 60°) were conducted using the PTR model and MODTRAN. Ozone calculations were taken in eight layers from 10 km to 25 km. For every case, through comparisons between the optical depths of these two models, a profile of absolute errors was obtained in every wavelength in the range of 0.3–0.8 μm. For ease of comparison, the RMS of the error profiles over all of the wavelengths for the six cases was calculated, and then an average error profile over six cases was obtained (Table 6). All RMSab were within 0.002. The water vapor calculations were taken in eight layers from 0 to 10 km. Similarly, average RMSab profile over six cases is listed in Table 6. All of the RMSab were within 0.0523. Good correspondences among the profiles calculated by these two models can be seen from the analysis.

4.4 *Comparison with LBLRTM*

The aforementioned comparisons and analyses of the accuracy of the PTR model refer to MODTRAN. To further examine the accuracy of the PTR model, the results of PTR were compared with LBLRTM. LBLRTM attributes provide spectral radiance calculations with accuracies consistent with the measurements against which they are validated and with computational times that greatly facilitate the application of the line-by-line approach to current radiative transfer applications (Clough et al., 2005). The ozone transmittances in the range of 0.3–0.8 μm and water vapor transmittances in the range of 0.568–4 μm for the USS atmosphere profile calculated using PTR were compared to those of LBLRTM. The detailed residual

Table 6. Average RMS error profiles over six cases for ozone and water vapor.

Ozone altitude (km)	Ozone RMSab (10^{-3})	Water vapor altitude (km)	Water vapor RMSab
10	1.29	0	0.0523
12	1.69	1	0.0292
14	1.77	2	0.0382
16	1.84	3	0.0311
18	1.9	4	0.0181
20	1.91	5	0.0163
22	1.83	6	0.0132
25	1.62	10	0.0071

curve for ozone (Fig. 7a) shows good agreement between these two models with a maximum absolute deviation of 0.0012. The residual curve for water vapor (Fig. 7b) shows that deviations as large as 0.15 can arise. The residual curve between MODTRAN and LBLRTM for water vapor is provided in Fig. 7c as well. The deviations between PTR and LBLRTM were mainly caused by the deviations between MODTRAN and LBLRTM. The substantial deviation occurs because the LBL model calculates in-band absorption by explicitly determining the spectral absorption of molecular on a fine spectral grid, while the result of the band model is approximated by a statistical representation of the number of lines and their strength, location, and overlap (Berk et al., 2004).

Although obvious residuals exist between LBLRTM and PTR, which are mainly caused by the intrinsic band formulation of band model, the residuals of transmittance calculation are acceptable when PTR is applied to solar heating rate (SHR) calculation. To test this point, the broadband SHR for the range 0.3–4 μm were calculated based on the transmittance calculated using PTR and LBLRTM, and the SHR results were compared. SHR was defined as the rate of temperature increase due to the solar radiation absorbed by the gases (Liou, 2002). The SHR for atmospheric layer between h_1 and h_2 is given by

$$\frac{\partial T}{\partial t} = \frac{\Delta F(h_1, h_2)}{\rho c_p \Delta h} , \tag{12}$$

where $\Delta F(h_1, h_2)$ is the difference between the net flux for h_1 and h_2, ρ is air density, c_p is specific heat at constant pressure, and Δh is the geometric thickness of the layer. The broadband net flux for PTR is calculated using the discrete ordinates radiative transfer model (DISORT) (Stamnes et al., 1988)

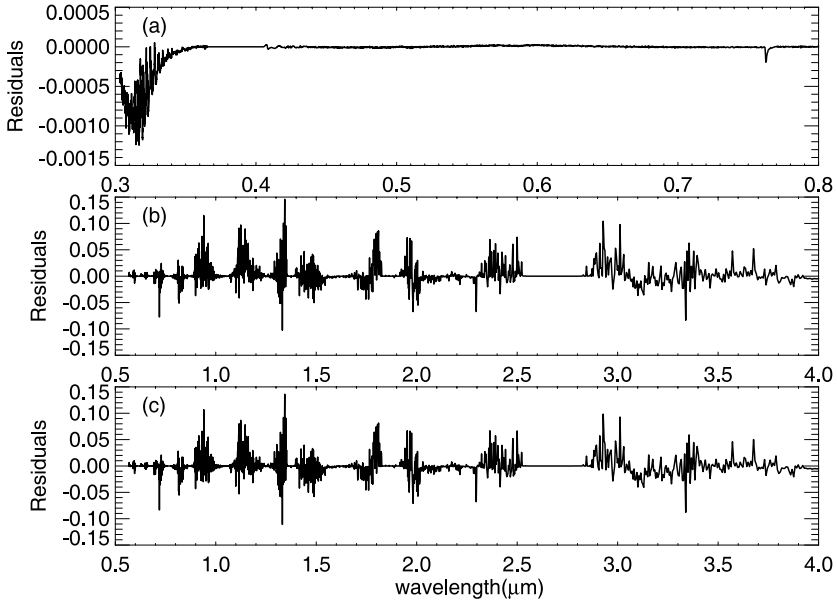

Fig. 7. Comparison of (a) ozone transmittance and (b) water vapor transmittance between PTR and LBLRTM (PTR-LBLRTM) and (c) water vapor transmittance between MODTRAN and LBLRTM (MODTRAN-LBLRTM).

while LBLRTM can calculate broadband net flux directly base on its precomputed transmittance. The SHR for three SZAs (21.5°, 45°, and 68.5°) for the USS atmosphere profile in 25 levels from 0 to 24 km with a resolution of 1 km were calculated and the absolute deviations between the SHR of PTR and LBLRTM as well as LBLRTM calculated SHR are shown in Fig. 8. The absolute deviation increased with decreasing SZA. When SZA decreases, the solar irradiance increases, and thus the SHR increases. The maximum deviations were 0.118 K d^{-1}, 0.214 K d^{-1}, and 0.238 K d^{-1} for SZAs of 68.5°, 45°, and 21.5°, respectively. The maximum deviation was 0.238 K d^{-1} for all cases; it occurred at 24 km when SZA was 21.5°; only 6% of the corresponding SHR was calculated using LBLRTM. These two models show better agreement in the lower atmospheric levels than in the upper levels. If we confine the comparison to troposphere, the deviations for all cases were within 0.08 K d^{-1}. All of the comparisons show that when applied to the SHR calculation, the PTR model shows good agreement with LBLRTM.

In fact, our preliminary calculations of transmittance for a few wavelengths (0.72 μm, 0.82 μm, and 0.94 μm) using LBLTRM show that the relationship between the calculated transmittance and SPL are the same as that shown in Fig. 1. So PTR can also be used to parameterize LBLRTM transmittances, and thus the new fitted transmittances in better agreement with LBLRTM results can be gained, which will be the concern of our future work.

4.5 *Computing speed comparison*

To examine the speed of the PTR model, the calculations of ozone and water vapor transmittances in 6166 wavelengths for the USS atmosphere profile when the SZA at 0° were repeated 600 times using the PTR model and MODTRAN, respectively. The processor used here was an Intel core 2 2.40GHz 4-core processor. The calculations of ozone transmittances take the PTR model 0.49 seconds, and the calculations of water vapor transmittances take 1.28 seconds, for a total of 1.77 seconds. The calculations take MODTRAN 114 seconds in all. The computational speed of PTR model is nearly two orders of magnitude faster than MODTRAN.

5. Conclusions

Absorption of ozone and water vapor in the solar-to-near-infrared band is climatically important due to their significant effects on the solar heating rate. Although many models such as MODTRAN and LBLRTM have been developed for the calculation of gas transmittance and have proven to be of great accuracy, an efficient parameterized model is still needed to improve computational efficiency. In this study, base on the transmittance data of MODTRAN, an efficient yet accurate parameterized model PTR used in the calculation of ozone and water vapor monochromatic transmittance in the solar-to-near-infrared spectrum

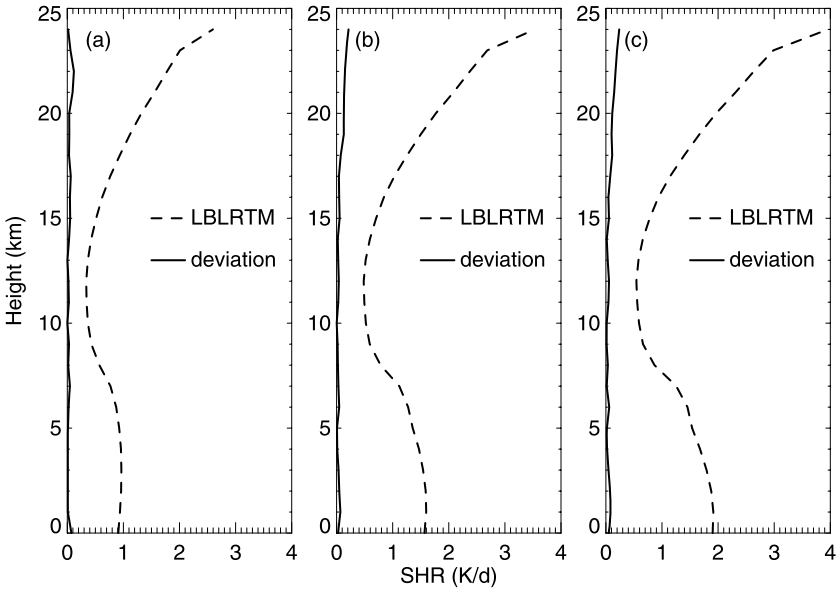

Fig. 8. Comparison of SHR calculated using PTR and LBLRTM for three different SZAs: (a) 68.5°, (b) 45°, and (c) 21.5° in the range of 0–24 km.

in the range of 0.3–4 μm with a spectral resolution of 5 cm^{-1} was developed using the least-squares method. Specifically, for every wavelength, the least-squares method was applied to find the best curve to represent the relationship between transmittance and SPL. Thus the polynomial equations used for parameterized transmittances calculation were derived.

Numerous comparisons were made between PTR and MODTRAN, taking MODTRAN as a reference. For ozone transmittance calculation, the overall RMSre was 0.823% for six atmosphere model cases. The RMSre was 0.374% when applied to the transmittance calculation for SAGE II ozone profiles. In all of the MFR and AERONET channels in the range of 0.3–0.8 μm, the RMSre were within 0.11%. For water vapor calculation, the overall RMSre was 8.48% for the six atmosphere models, while for the transmittance range of 1×10^{-3}–1 this error was reduced to 3.48%. The RMSre was 7.92% when the transmittance calculation for UWYO water vapor profiles was used. In all of the AERONET and MODIS channels in the range of 0.568–4 μm, the RMSre were within 2.34%. To evaluate the accuracy of PTR in different heights, the optical depth profiles were calculated using PTR were also compared with the results of MODTRAN, and comparisons show that RMSab for all of the heights were within 0.002 for ozone and within 0.0523 for water vapor. All of the comparisons showed good agreement between PTR and MODTRAN. To examine the efficiency of PTR model, the computational speeds of the PTR model and MODTRAN were compared. The PTR model was found to be nearly two orders of magnitude faster than MODTRAN.

Because the PTR model was developed base on MODTRAN calculations, to further evaluate the accuracy of PTR, the comparison between PTR and LBLRTM was conducted. For the ozone transmittance calculation, these two models agreed very well, with a maximum deviation of 0.0012. For the water vapor transmittance, the deviation was as large as 0.15 and was mainly caused by the intrinsic band formulation of band model. However, these deviations are acceptable in the calculation of solar heating rate, which can be testified by comparing the solar heating rates calculated based on the transmittances of PTR and LBLRTM. The solar heating rates for PTR transmittances in the 0.3–4 μm band in the range of 0–24 km were in good agreement with those for LBLRTM transmittances, with a maximum absolute deviation of 0.238 K d^{-1} (6% of corresponding solar heating rate calculated using LBLRTM). These two models show better agreement in the lower atmospheric levels than in the upper levels. In the troposphere, all of the deviations were within 0.08 K d^{-1}. All of these comparisons indicate that the PTR model is an accurate yet efficient model that can be widely used in solar heating rate calculation in climate models.

Acknowledgements. This work was supported by the National Basic Research Program of China (Grant No. 2011CB403401) and the National Natural Sciences Foundation of China (Grant No. 41175029).

REFERENCES

Berk, A., and Coauthors, 2004: MODTRAN5: A reformulated atmospheric band model with auxiliary species and practical multiple scattering options. Rep. BS-HA-TR-2004-1139, Air Force Geophys. Lab., Bedford, MA.

Clough, S. A., M. W. Shephard, E. J. Mlawer, J. S. Delamere, M. J. Iacono, K. Cady-Pereira, S. Boukabara, and P. D. Brown, 2005: Atmospheric radiative transfer modeling: A summary of the AER codes, short communication. *Journal of Quantitative Spectroscopy and Radiative Transfer*, **91**, 233–244.

Collins, W. D., J. K. Hackney, and D. P. Edwards, 2002: An updated parameterization for infrared emission and absorption by water vapor in the National Center for Atmospheric Research Community Atmosphere Model. *J. Geophys. Res.*, **107**(D22), 4664, doi: 10.1029/2001JD001365.

Fu, Q., and K. Liou, 1992: A three-parameter approximation for radiative transfer in nonhomogeneous atmospheres: Application to the O_3 9.6-μm band. *J. Geophys. Res.*, **97**(D12), 13051–13058.

Harrison, L. C., J. J. Michalsky, and J. Berndt, 1994: Automated multifilter rotation shadowband radiometer: An instrument for optical depth and radiation measurements. *Appl. Opt.*, **33**, 5188–5125.

Holben, B. N., and Coauthors, 1998: AERONET—A federated instrument network and data archive for aerosol characterization. *Remote. Sens. Environ.*, **66**, 1–16

Kiehl, J. T., and S. Solomon, 1986: On the radiative balance of the stratosphere. *J. Atmos. Sci.*, **43**, 1525–1534.

Kneizys, F. X., and Coauthors, 1988: Users Guide to LOWTRAN 7. Rep. AFGL-TR-88-1077, Air Force Geophys. Lab., Bedford, MA, 137pp.

Kratz, D. P., and R. D. Cess, 1988: Infrared radiation models for atmospheric ozone. *J. Geophys. Res.*, **93**, 7047–7054.

Liou, K. N., 2002: *An Introduction to Atmospheric Radiation*. 2nd ed., Elsevier, 583pp.

Mauldin, L. E. III, N. H. Zaun, M. P. McCormick, J. H. Guy, and W. R. Vaughn, 1985: Stratospheric Aerosol and Gas Experiment II instrument: A functional description. *Optical Engineering*, **24**, 307–312.

Ou, S.-C., and K.-N. Liou, 1983: Parameterization of carbon dioxide 15μm band absorption and emission. *J. Geophys. Res.*, **88**, 5203–5207.

Rosenfield, J. E., 1991: A simple parameterization of ozone infrared absorption for atmospheric heating rate calculations. *J. Geophys. Res.*, **96**(D5), 9065–9074.

Rothman, L. S., and Coauthors, 2005: The HITRAN 2004 molecular spectroscopic database. *Journal of Quantitative Spectroscopy and Radiative Transfer*, **96**, 139–204.

Stamnes, K., S.-C. Tsay, W. J. Wiscombe, and K. Jayaweera, 1988: Numerical stable algorithm for discrete-ordinate-method radiative transfer in multiple scattering and emitting layered media. *Apllied Optics*, **27**, 2502–2509.

Yang, J. M., and J. H. Qiu, 2002: A method for estimating precipitable water and effective water vapor content from ground humidity parameters. *Chinese J. Atmos. Sci.*, **26**, 9–22.

Young, A. T., 1994: Air mass and refraction. *Applied Optics*, **33**, 1108–1110.

Zhong, W. Y., and J. D. Haigh, 1995: Improved broadband emissivity parameterization for water vapor cooling rate calculations. *J. Atmos. Sci.*, **52**, 124–138.